Analysing and Classifying VLF Transients

Ernst D. Schmitter

Abstract— Monitoring lightning electromagnetic pulses (sferics) and other terrestrial as well as extraterrestrial transient radiation signals is of considerable interest for practical and theoretical purposes in astro- and geophysics as well as meteorology. Managing a continuous flow of data, automation of the analysis and classification process is important. Features based on a combination of wavelet and statistical methods proved efficient for this task and serve as input into a radial basis function network that is trained to discriminate transient shapes from pulse like to wave like. We concentrate on signals in the Very Low Frequency (VLF, 3 -30 kHz) range in this paper, but the developed methods are independent of this specific choice.

Keywords— transient signals, statistics, wavelets, neural networks

I. INTRODUCTION

ATMOSPHERIC electromagnetic pulse radiation (shortly sferics) related to thunderstorms is a subject of continuous monitoring within worldwide networks for some decades with purposes going from early warnings for severe weather conditions via geophysical research to psychobiological studies [1], [2], [3]. But there is a lot more natural transient electromagnetic activity from terrestrial as well as extraterrestrial sources [7]. In the last years transient radiation on different time scales from earth crust zones under severe pressure is under consideration in the context of earthquake precursors [4],[5],[6]. Characterising, discriminating and classifying natural transient signals therefore is a task with possibly far reaching applications in very different disciplines.

Amplitude thresholding and exact correlation with time of a properly identified pulse at various receiving places is sufficient for localising the signal source. For sferics automated location and intensity logging is practised successfully with increasing accuracy within networks.

Automatic discrimination of transient signal shapes for further investigations needs some more envolved methods we want to discuss in this paper.

We concentrate upon typical transients received in the VLF range (by definition 3 .. 30kHz, sferics usually have highest amplitudes between 1.5 and 15 kHz). These are: unipolar pulses (from very different sources, partly man made, Fig. 1), bipolar pulses (mostly caused by man made switching events) sferics (lightning radiation with ionospheric echoes, Fig. 2), slow tailed sferics (presumably caused by lightnings followed by a continuous current flow; these events are suspected to cause sprites, i.e. voluminous discharges above a thunderstorm up to the lower ionosphere, Fig. 3), tweaks (prolongued, ionospherically dispersed sferics, Fig. 4, they produce a tweaking sound if fed to an audio system) and damped oscillations of mostly man made origin (Fig. 5).

Ernst D. Schmitter is with the University of Applied Sciences Osnabrueck, 49076 Osnabrueck, Germany, (phone +49 541 9692093; email: e.d.schmitter@fh-osnabrueck.de)
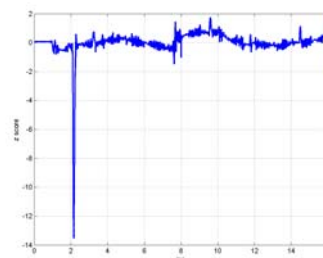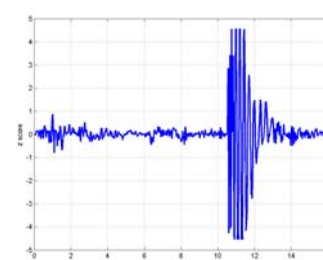
Fig. 1: Unipolar pulse

Fig. 2: Sferic: lightning transient with ionospheric echoes

II. SHAPE FEATURES OF TRANSIENTS

A. Statistics based features

Usually amplitude thresholding is the first step filtering out strong signals. After that, some information about the transient shape can be quantified using the signal value distribution. For further processing, the signal $y(i)$ is normalised, i.e. its z-scores are calculated:

$$z(i) = \frac{y(i) - \mu}{\sigma} \qquad (1)$$

Normalised signals of different sources can be compared more easily. Together with the mean μ and the standard deviation σ the signal $y(i)$ can be reconstructed from the $z(i)$. $z(i)$ is the dimensionless deviation of $y(i)$ from the mean as a multiple of the signal standard deviation. Fig. 6 shows the corresponding z-score histogram to fig. 2.

For shape characterisation we use the 3rd and 4th moments of the distribution, i.e. skewness sk and kurtosis ku:

$$sk = \frac{1}{n} \sum_{i=1}^{n} z(i)^3 \qquad (2)$$

$$ku = \frac{1}{n} \sum_{i=1}^{n} z(i)^4 - 3 \qquad (3)$$

Skewness is sensitive to unipolarity of the signal. For example a large negative skewness usually is a consequence

World Academy of Science, Engineering and Technology
International Journal of Geological and Environmental Engineering
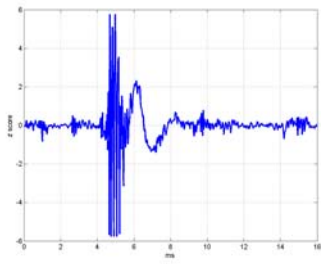Vol:1, No:6, 2007

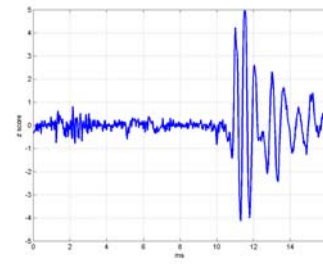Fig. 3: Sferic with slow tail

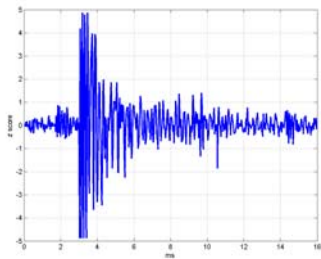Fig. 5: Damped oscillation

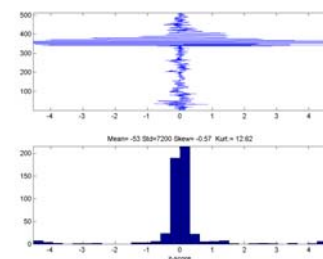Fig. 4: Tweak: ionospherically dispersed sferic

Fig. 6: Normalised signal value distribution (Fig. 2)

of a large negative pulse. Kurtosis is a measure of how tailed the distribution is. A large positive value indicates a strongly 'leptokurtic' distribution shape i.e. values are concentrated around the mean with large (but rare) outliers produced by bipolar pulses in the signal - in contrast e.g. to a gaussian bell shaped distribution with about zero kurtosis as we have with oscillations and noise. A broadened ('platykurtic') histogram shape is characterised by negative kurtosis.

B. Wavelet transform based features

Discrete wavelet transformations (DWTs) have proved to be a valuable tool for transients characterisation.

Fig. 8 shows a signal train ($2^9 = 512$ components, 16 ms at 32 kHz sampling rate) containing a sferic (cp. Fig. 2) with its DWT sum and detail coefficients with respect to the highly localised Daubechies (DAUB4) wavelets [11].

In fig. 7 the typical steps of a discrete wavelet transform algorithm in the case of a Daubechies (4 coefficient) transform are reviewed. The action of the DWT matrix D on an example signal vector $\vec{y} = (y_1..y_8)$ gives as the first coefficient of the result vector: $D\vec{y}(1) = s1 = c_1 * y_1 + c_2 * y_2 + c_3 * y_3 + c_4 * y_4$, which with positive coefficients c_i is a weighted sum of the first 4 signal values. $D\vec{y}(2) = d1 = c_3 * y_1 - c_2 * y_2 + c_1 * y_3 - c_0 * y_4$ is a weighted difference of the first 4 signal values. Thus $D\vec{y}$ alternatingly contains moving weighted averages and differences of the input signal. The exact values of the coefficients are fixed by imposing the following requirements, cp. [11]:

D should be orthogonal: $DD_+ = Id$, so $D^{-1} = D^+$. The difference operation should yield 0 in case of a constant signal: $c_3 - c_2 + c_1 - c_0 = 0$ as well as for a linearly increasing signal: $c_3 * 0 - c_2 * 1 + c_1 * 2 - c_0 * 3 = 0$.

The 4 sums are then gathered in the upper part and the differences in the lower part of a new vector. The reduced matrix D (4x4) is then applied in the same manner to the upper part only. This scheme is repeated q-1 times for a vector of length 2^q and generates q detail scales. So for 8 values ($q = 3$) in two steps 3 scales are generated or for 512 values 9 detail scales in eight steps.

For the detection of the relevant signal features the energies in the different DWT scales have been proved to be useful. The energy $e(s)$ on scale s simply is the squared sum of the DWT coefficients of that scale.
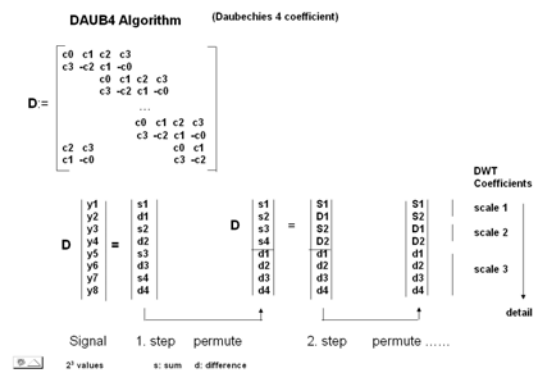

Fig. 7: Discrete wavelet transformation scheme for the Daubechies 4 coefficient case.

Filtering out the slow components of a signal is an efficient way to find out its pulse characteristics - in contrast to other applications, where the fast varying part is unwanted 'noise'.

Looking at the frequency domain, zeroing more and more of the less detail ('slow') coefficients increasingly attenuates the lower frequency amplitudes - fig. 9.

World Academy of Science, Engineering and Technology
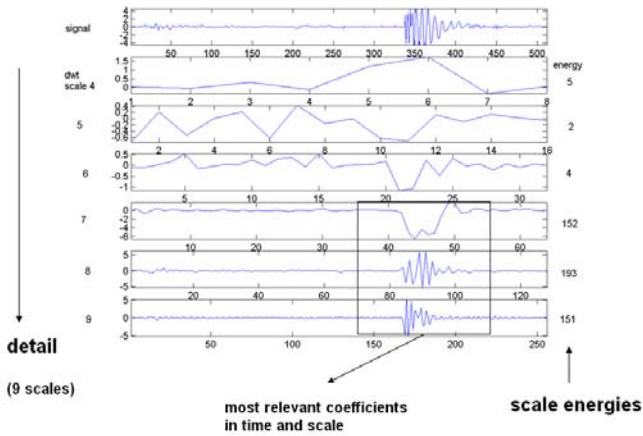International Journal of Geological and Environmental Engineering
Vol:1, No:6, 2007

Fig. 8: Input signal and discrete wavelet coefficients from coarse (slow) to detailed (fast) scales and the scale energies (right). Only the coefficient ranges with highest scale energies are kept for areconstruction of the transient (local filtering).
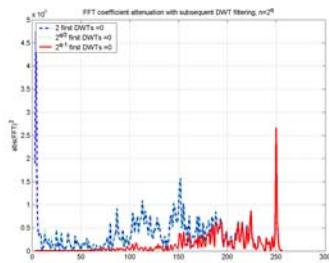
Fig. 9: Subsequent attenuation of low frequency amplitudes with DWT fast component filtering

The main advantage of wavelet transforms over Fourier and related transforms however is its locality. So by transforming back only those DWT coefficients localised near the time event of interest isolates just the transient under investigation. Because of taking into account local coefficients on the scales with the highest energy, more details of the pulse are reconstructed as with a simple fast component filtering using only the coefficients of the most detailed scale or a high pass Fourier filter.

Fig. 10 shows the relevant part of a locally filtered transient. It was gained by an inverse wavelet transform of the 3 scales with the highest energies restricted to the time span where the signal is above a threshold. The time distance of the ionospheric echoes converges to $\Delta t = 2h/c$, with h the height of the reflecting lower ionospheric boundary and the velocity of electromagnetic radiation, c. With $\Delta t = 1/3 \ ms$ for this wave packet, $h = 50 km$.

III. CLASSIFICATION WITH A RADIAL BASIS FUNCTION NEURAL NETWORK (RBFN)

Signal skewness and kurtosis, i.e. the 3rd and 4th moments of the value distribution together with the energies of the wavelets scales form a feature vector suitable for classification.
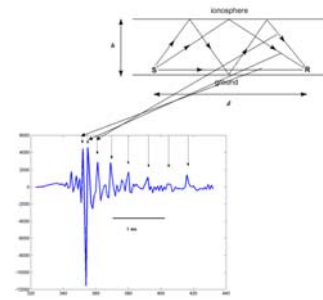

Fig. 10: Locally component filtered signal and identification of ionospheric echoes.

In our example each signal has $512 = 2^9$ components (using 32000 samples/sec this results in a duration of 16ms). The energies of the DWT scales 2..9 are used for the feature vector that in total has 10 components as inputs for the classifier. The task of the classifier using this feature vector is to discriminate unipolar pulses (output center value $y = +1$), sferics ($y = 0.5$), slow tailed sferics ($y = 0.0$), tweaks ($y = -0.5$), and oscillations ($y = -1$), i.e. from 'pulse like' to 'wave like', so that events can be automatically sorted and saved for further analysis. The sequence of transients as just indicated can be characterised by a continuous classification parameter going from 'pulse like' to 'wave like'.

A radial basis function network (RBFN, [12]) with a 10 parameter feature input and a single output parameter is trained with a set of training vectors (see Fig. 11).
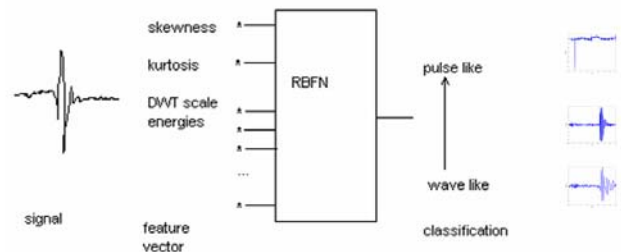

Fig. 11: Signal classification scheme

Each training vector consists of 10 features and a classification value y. The matrix of training vectors is normalised with respect to the mean and the standard deviation of each component. With normalised feature vector $\vec{x}$, K weights w_j, basis function centers $\vec{t}_j$ and width parameters c_j the normalised classification output $y^{(n)}$ for a (normalised) input $\vec{x}$ is

$$y^{(n)}(\vec{x}) = \sum_{j=1}^{K} w_j e^{-c_j (\vec{x} - \vec{t}_j)^2} \qquad (4)$$

As starter parameters for a training process we randomly select K basis function centers $\vec{t}_j$ from the training set and define constant width parameters

World Academy of Science, Engineering and Technology
International Journal of Geological and Environmental Engineering
Vol:1, No:6, 2007

$$c_j := \frac{K}{d_{max}^2} \tag{5}$$

with the maximum center distance

$$d_{max} = max_{i,j}|\vec{t}_i - \vec{t}_j| \tag{6}$$

The initial weights we get from

$$w_j := \sum_{i=1}^{m} g_{ji}^+ y_i^{(n)} \tag{7}$$

with m training vectors $(\vec{x}_i, y_i^{(n)})$, and g^+ being the pseudoinverse matrix of $g_{ij} := e^{-c_j(\vec{x}_i - \vec{t}_j)^2}$.

Weights, centers and width parameters are then optimised (trained) using a Nelder-Mead-simplex algorithm [11] with respect to the mean squared classification error.

We usually use $K = 10$ basis functions with several hundreds of training vectors. The main problem with getting enough proper training vectors is, that for example normal sferic transients occur abundantly frequent, whereas others occur quite rarely. In a VLF monitoring system the RBFN is successfully used to automatically sort the flow of incoming amplitude thresholded signal chunks into the mentioned transients classes. The fuzzy transition between the transients is satifactorily reflected by the continuous output parameter. Wrong classifications (i.e. with an y-error > 0.5) occur in less than 5 % of the received samples.

Fig. 12 shows the graphical user interface of a software implementation of the described transient analysis and classification algorithms. An incoming transient is shown together with its fast Fourier transform. In the lower left the component values of the feature vector generated by this signal are displayed. These are input values for the RBFN. The last number in this row following the input values is the output of the RBFN times 100.

Fig. 13 is an example for a fast scale analysis of the same incoming wavefrom as in fig. 12. After zeroing out slow scale DWT coefficients and back transformation the resulting transient is shown.

The Multi Media control box in the lower right of the user interface allows to hear the sound of the transient as the VLF frequency range largely overlaps with the audio frequency domain.

At this place we would like to thank Michael Hebert, Honolulu, for initiating the development of this time domain receiver software and for many helpful online discussions.

IV. Fuzzy Rule Interpretation of the RBFN

One of the reasons for choosing a RBFN was, that it has a structure allowing a straightforward Takagi-Sugeno fuzzy rule interpretation [13], [14], [15] for each member function:

IF $\vec{x}$ is in the domain of basis function j THEN $y^{(n)} = w_j$

So, the RBFN output (equ. 4) can equivalently be looked at as the output of a system with K rules, each having fuzzy premises and crisp consequences. In this context w_j is the
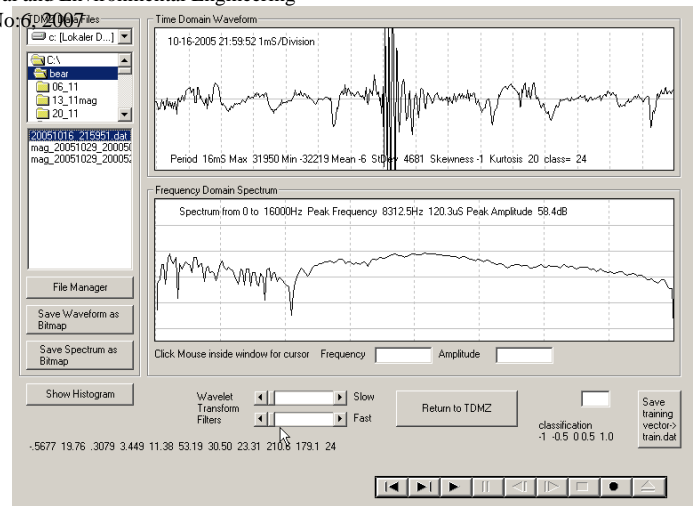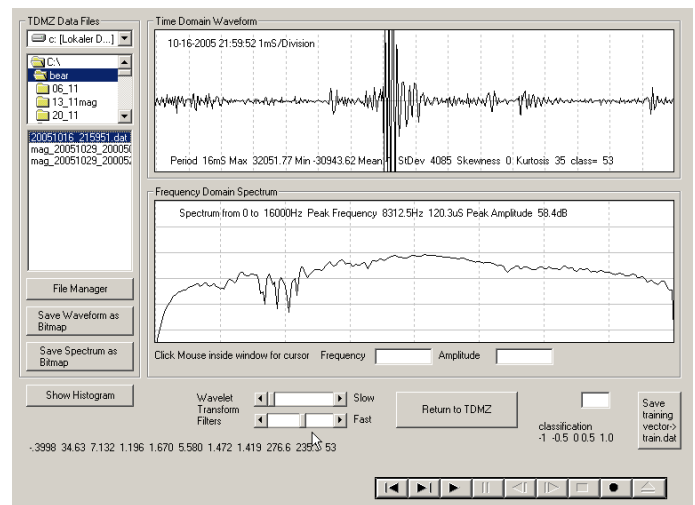

Fig. 12: Transients analysis and classification software

Fig. 13: Transients analysis and classification software: wavelet filtered sferic (discarding coarse scales)

weight of rule j and $e^{-c_j(\vec{x} - \vec{t}_j)^2}$ the relevance of rule j.

Because of

$$e^{-c_j(\vec{x} - \vec{t}_j)^2} = e^{-c_j(x_1 - t_{j1})^2} e^{-c_j(x_2 - t_{j2})^2} .. e^{-c_j(x_p - t_{jp})^2} \tag{8}$$

for a p-dimensional input the premise part of rule j can be read as

IF x_1 is in d_{j1} AND x_2 is in d_{j2} .. AND x_p is in d_{jp}

where $d_{ji} = e^{-c_j(x_i - t_{ji})^2}$ is the gaussian membership function for input i centered at t_{ji} with width parameter c_j.

We should add, that the usual RBFN corresponds to a reduced Takagi-Sugeno fuzzy model. In general, T-S fuzzy rules have the form:

IF x_1 is in d_{j1} AND x_2 is in d_{j2} .. AND x_p is in d_{jp}
THEN $y^{(n)} = w_{j0} + w_{j1}x_1 + w_{j2}x_2 + .. + w_{jp}x_p = w_{j0} + \vec{w}_j \cdot \vec{x}$

World Academy of Science, Engineering and Technology
International Journal of Geological and Environmental Engineering
Vol:1, No:6, 2007

Replacing w_j by $w_{j0} + \vec{w}_j \cdot \vec{x}$ in the RBNF output (equ. 4) generalises the RBNF to a locally linear RBNF, also called Locally Linear Neuro Fuzzy Model (LLNFM). An efficient iterative training procedure for LLNFMs called LOLIMOT (LOcally LInear MOdel Tree) is described in [16]. Within this framework there is an additional number of $K * p$ free parameters that can help to reduce the total number of rules K and by this easing a fuzzy rule interpretation.

Fuzzy rule based interpretation of a RBFN with a moderate number of basis functions allows for some more direct insight into the classification process, than e.g. backpropagation networks. In this way domain analysis of the basis functions using the trained centers, widths and weights reveals correlations between feature combinations and transients characteristics. Future work is going in this direction.

V. CONCLUSION

A sequence of statistics and wavelet transform based features proved useful with automating transients signal detection, classification and analysis. Whereas the moment parameters skewness and kurtosis characterise global signal distribution statistic properties, the wavelet scale energies represent information about the behaviour at different time scales.

Using a radial basis function net, the features successfully discriminate transients received in the VLF frequency range from 'pulse like' to 'wave like'.

The sets of the wavelet coefficients with the highest energy contents additionally provide the information to locally reconstruct the most relevant part of the transient for further analysis.

The transients shown in this paper have been monitored with an E-field receiver, the signal then fed into the sound card of a notebook and digitally processed with the described algorithms in this paper - thus providing a mobile VLF monitoring, discrimination and analysis system. We believe that the discussed methods are valuable beyond this example.

REFERENCES

[1] Betz H.-D., Oettinger W. P., Schmidt K., Wirz M., Modern Lightning Detection and Implementation of a New Network in Germany, General Assembly EGU, Wien/ Austria, April 2005
[2] Betz H.-D., Eisert B. , Oettinger W. P., Four year experience with an atmospherics-based automatic early warning system for thunderstorms, Proc. 26th Int. Conference on Lightning Protection (ICLP), Cracow/ Poland, 91-95, ISBN 83-910689-5-1, 2002
[3] Schienle A., Stark R., Walter B., Vaitl D., Kulzer R., Effects of Low-Frequency Magnetic Fields on Electrocordical Activity in Humans: A Sferic Simulation Study, International Journal of Neuroscience, 90, 21-36, 1997.
[4] Tzanis, A., Vallianatos, F., A critical review of Electric Earthquake Precursors, Annali di Geofisica, 44/2, 429-460, 2001
[5] Konstantanaras, A., Varley, M.R., Vallianatos, F., Collins, G., Holifield, P., A neuro-fuzzy approach to the reliable recognition of electric earthquake precursors, Natural Hazards and Earth Sciences 4:641-646, 2004
[6] Steinbach, P., Lichtenberger, J., Ferencz, Cs., Case studies of possible earthquake related perturbations on narrow band VLF time series, Geophysical research abstracts, Vol. 5, 10946, 2003
[7] Aschwanden, M., Kliem B., Schwarz U., Kurths, J., Wavelet Analysis of Solar Flare Hard X-rays, The Astrophysical Journal, 505:941, 1998, October 1
[8] Cummer, S.A.,Lightning and ionospheric remote sensing using VLF/ELF radio atmospherics, Dissertation. Stanford University. August 1997
[9] Reising, S.C., Remote sensing of the electrodynamic coupling between thunderstorm systems and the mesosphere / lower ionosphere. Dissertation. Stanford University. June 1998
[10] Mushtak V.C., Lowenfels D.F., Williams E.R., Stewart M.F., Full ELF/VLF Bandwitdh Observations of Lightning in the Earth-Ionosphere Waveguide, American Geophysical Union, Fall Meeting 2002, abstract A11C-0111
[11] Press W.H., Teukolsky S.A., Vetterling W.T., Flannery B.P., Numerical Recipes in C, Cambridge University Press, 1992
[12] Haykin, S., Neural networks, Prentice Hall, 1999
[13] Takagi, T., Sugeno, M., Fuzzy identification of systems and its applications to modeling and control, IEEE Transactions on Systems, Man and Cybernetics, vol. 15, 116-132, 1985
[14] Jang, S.R., Sun, C.T.,Functional equivalence between radial basis function networks and fuzzy inference, IEEE Transctions on neural networks, 4(1), 156-159, 1993
[15] Jin, Y., Sendhoff, B., Extracting interpretable fuzzy rules from RBF networks, Neural Processing Letters, 149-164, 2003
[16] Nelles, O., Nonlinear System Identification, Springer, Berlin, 2001